Supplementary Information

In the metal-amplified density assay (MADA), all the beads levitated at the same height in the developing buffer initially regardless of the concentration of gold-labeled protein that the beads were exposed to, suggesting that MagLev, at least in the form we implemented, was not able to detect the binding of gold nanoparticles onto the surface of the beads. The beads however, changed levitation height in the buffer differently depending on the concentration of gold-labeled protein that the beads were exposed to. The dependence on the rate of change of the levitation height on the amount of gold-labeled protein, allowed, when we used gold-labeled antibody in the detection step, to perform immunoassay with antibodies and antigens (DeLISA). We obtain a minimal model for the dependence of the change in levitation height to the concentration of gold-labeled protein in solution by adapting models developed in the early 1980s for the electrochemical deposition of metals onto electrodes [1–3]. The model captures the scaling of the time dependence of the change in levitation height of the beads and demonstrates that the change of levitation height depends on the number of nanoparticles adsorbed on the surface of the bead and the surface to volume ratio of the bead.

The Supplementary Information is organized as follows. In Section I we report measurements using ICP-MS of the amount of gold present on the surface of the beads due to the binding of gold-labeled streptavidin to biotin-labeled beads. We obtained the binding isotherm by converting the mass data into the number of bound nanoparticles on the surface of the beads. In Section II we develop the model for the growth of the nanoparticles on the surface of the bead. In Section III we rederive the equations for the levitation height of small beads (of arbitrary shape) in the MagLev device from Subramaniam et. al [4], and in IV we modify the equation to take into account the change in the density of the bead due to the binding and growth of the gold-nanoparticle labeled proteins.

I. ICP-MS MEASUREMENTS OF THE AMOUNT OF GOLD ON BEADS DUE TO THE BINDING OF GOLD-LABELED STREPTAVIDIN

Fig.S1 shows schematically the procedure we used to quantify the number of gold-labeled streptavidin molecules adsorbed onto the surfaces of the beads. Seven beads were placed

in a known volume of aqua regia. The dilute aqua regia dissolved the metallic gold on the surface of the beads to yield gold ions in solution. The concentration of gold ions were then quantified with ICP-MS.

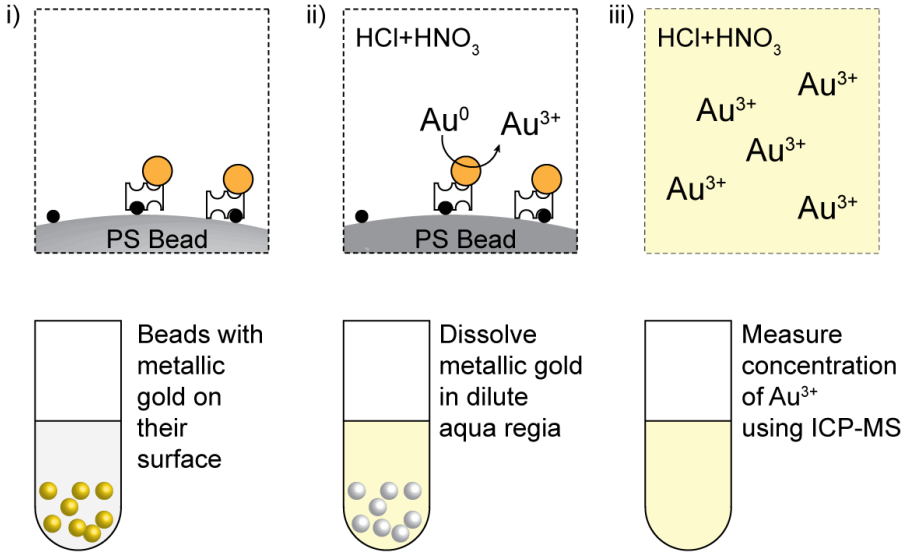

Fig. S1. Schematic of procedure for measuring the amount of gold deposited onto the beads.

1. *Binding characteristics of gold-labeled streptavidin to biotin-labeled beads*

We exposed seven biotin labeled beads each to varying concentrations of gold-labeled streptavidin and then quantified the amount of gold that was present on the surface of the beads. Fig. S2A shows a plot of the concentration of Au^{3+} versus the concentration of free gold-labeled streptavidin in the sample. It is clear that the concentration of Au^{3+} released from the surface of the beads increased as a function of the concentration of gold-labeled streptavidin in solution. We converted the concentration data into the number of nanoparticles using Equation 1.

$$N_0 = \frac{[Au^{3+}]V_{AR}}{N_B \frac{4}{3}\rho_{Au}\pi r_{np}^3} \tag{1}$$

In this equation V_{AR} is the volume of aqua regia used to dissolve the gold, $N_B = 7$ is the number of beads used, $r_{np} = 5$ nm is the radius of the nanoparticles, and $\rho_{Au} = 19.3$ g/cm^3

is the density of gold.

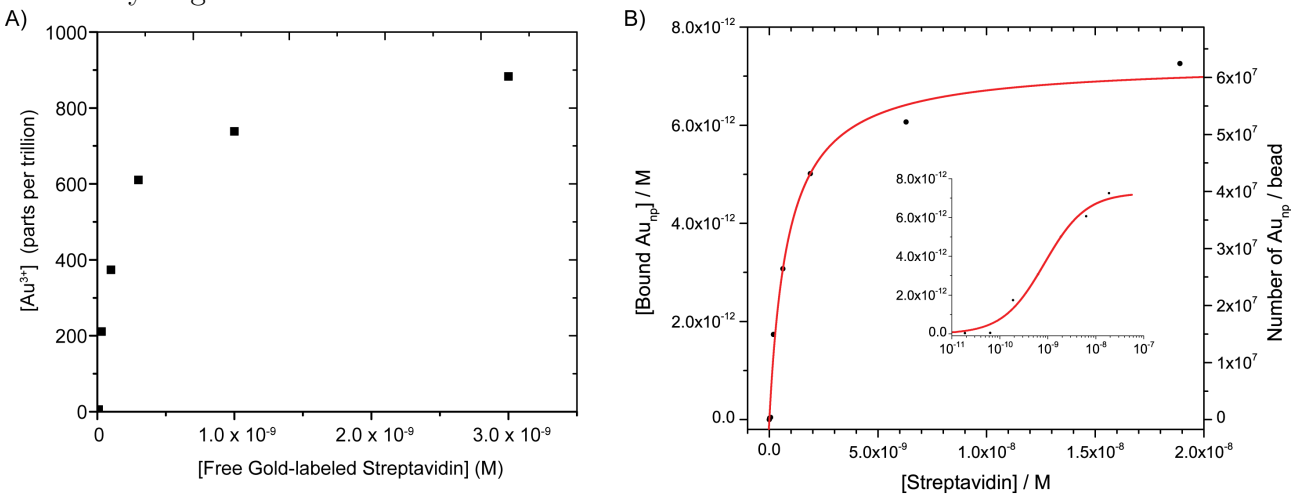

Fig. S2. The binding isotherm of gold-labeled streptavidin to biotin-labeled beads. A) Plot showing the concentration of gold released from the beads into the dilute aqua regia vs the concentration of free gold-labeled streptavidin that the beads were exposed to. B) Plot showing the concentration of surface bound gold nanoparticles vs the the concentration of free gold-labeled streptavidin. The red continuous lines are fits of Eq. 4 to the data. The inset show the binding isotherm on a semi-log scale.

Fig. S2b shows the concentration of gold nanoparticles, $[Au_{np}]$, bound to the surface of the bead versus the concentration of free gold-labeled streptavidin in solution. The right axis shows the number of particles per bead. The inset shows the data plotted with the x-axis on a log scale.

Streptavidin is capable of binding four biotin molecules in solution [5, 6]. To model our data, we make the assumption that one streptavidin protein binds to a single biotin ligand. We return to this assumption later in this section to show that this assumption is valid within the context of our system. With this assumption, we apply the Law of Mass action to obtain a relation between the concentration of nanoparticles bound to the surface, [SB] versus the concentration of free gold-labeled streptavidin [S] (Equation 2). [B] is the concentration of biotin on the surface of the beads, which is not known *a priori*.

$$[\mathrm{S}] + [\mathrm{B}] \underset{\mathrm{k_d}}{\overset{\mathrm{k_a}}{\rightleftharpoons}} [\mathrm{SB}] \tag{2}$$

In this equation k_a and k_d are the association and dissociation rate constants, respectively. The equilibrium dissociation constant K_d is given by Equation 3.

$$K_d = \frac{k_d}{k_a} = \frac{([S]_0 - [SB])([B]_0 - [SB])}{[SB]} \tag{3}$$

In this equation $[S]_0$ is the initial concentration of streptavidin in the sample and $[B]_0$ is the total concentration of immobilized biotin ligands. We solve for the concentration of immobilized complex $[SB]$ to obtain Equation 4.

$$[SB] = \frac{[S]_0 + [B]_0 + K_d}{2} - \sqrt{\frac{([S]_0 + [B]_0 + K_d)^2}{4} - [S]_0[B]_0} \tag{4}$$

We fitted Equation 4 to our experimental data in the nonlinear least square sense using the curve fitting program Origin Pro (version 8.5, OriginLab) to determine the two unknown parameters K_d and $[B]_0$. The equation fitted the data well (red continuous lines). The value of $K_d = 8.5 \times 10^{-10}\mathrm{M}^{-1}$ compared favorably with measurements done on other systems of the binding of biotin to streptavidin modified surfaces [7, 8].Note that conjugation of streptavidin with fluorophores, DNA, or solid surfaces decreases the K_d by about 4-5 orders of magnitude below the measured $K_d \approx 10^{-14}M^{-1}$ of biotin interacting with free streptavidin in solution [7, 8]. In contrast, antibodies have K_d that range from $10^{-6}\mathrm{M}^{-1}$ to $10^{-12}\mathrm{M}^{-1}$ [9].

As an additional check, we calculated the distance between biotin binding sites on the surface of the beads. Our fitted value to the data indicated that the number of biotin molecules on the surface was 6.4×10^7. For beads with a diameter of 600 micrometers with an area of 1.13×10^{-6} m^2, that leads to a surface density of 1.77×10^{-14} biotin molecules/m^2. We take the square root of this value to estimate the distance between the biotin molecules to be of the order of 130 nm.

Since a streptavidin molecule is about 5 nm in diameter $\ll$ 130 nm; a single streptavidin molecule can bind only to one biotin molecule on the surface. Furthermore, since the gold nanoparticles are 10 nm in diameter, each gold nanoparticle can only be bound to on average one biotin binding site; nanoparticles bridging two biotin binding sites is highly unlikely. We thus conclude that it is reasonable to use the Law of Mass Action to model the equilibrium

dynamics of gold-labeled streptavidin to biotin labeled beads.

II. KINETICS OF GROWTH OF THE NANOPARTICLES IN THE DEVELOPING BUFFER

The rate of growth of the nanoparticles that are adsorbed on the surface of the beads in the developing buffer determines the rate of change of the levitation height of the beads in the MagLev device. We wished to thus obtain a model of the growth of the nanoparticles.

In a MADA, $N_0 = NS$ (N_0 is the total number of nanoparticles, N is the number of nanoparticles per unit area (number/m^2), and S is the total surface area of the bead (m^2)), gold nanoparticles are immobilized onto the surface of beads through specific biomolecular recognition events. The number of nanoparticles on the surface of the bead varies with the concentration of analyte that was present in the sample being assayed. In the developing buffer, these nanoparticles serve as nuclei that catalyze the deposition of metallic gold from solution onto the bead. Physically, the nanoparticles increase in volume as metal deposits on their surfaces. This process is typically diffusion-limited. As the radius of the nanoparticles increase, neighboring nanoparticles eventually touch (Fig. 3A in the main text). Further growth leads to the formation of a film of gold on the surface of the bead.

The mass flow rate of reactants, $\dot{m}$ (kg/s) due to the diffusion-limited growth of a hemispherical nucleus is given by equation 5[1–3]. The boundary conditions are $c(\infty, t) = \bar{c}$, $c(0, t) = 0$ (ions are instantaneously reduced on the surface of the nanoparticle). In this equation, $c(r, t)$ is the concentration of reactant (for simplicity we assume [Au^{3+}]) and $\bar{c}$, (mol m^{-3}) is the bulk concentration of reactant.

$$\dot{m}_1 = \frac{(2DcM)^{3/2} t^{1/2}}{\rho^{1/2}} \tag{5}$$

In this equation, ρ is the density of the deposited material (kg m^{-3}), M is the molar mass of the deposit (kg mol^{-1}), and D is diffusion coefficient of the reactant (m^2 s^{-1}).

For an array of N nuclei growing independently on a flat surface, the net mass flow rate is given by a sum of the mass flow rates to each nuclei (Equations 6, 7).

$$\dot{m}_N = \sum_{1}^{N} \dot{m}_i \tag{6}$$

$$\dot{m}_N = \frac{N\pi(2DcM)^{3/2}t^{1/2}}{\rho^{1/2}} \tag{7}$$

In a MADA, the number of nanoparticles on the surface could be of high enough density that the growing particles interact with each other. The competition for reactants by the growing nanoparticles results in locally lower concentration of reactants to the growing nuclei. The lower concentration could lead to a slower growth rate than that expected from equation 7.

Following [1–3] a hemispherical 'diffusion' zone radiating from a nanoparticle grows at a radial velocity such that its radius, $l(t)$, is described as a function of time by Equation 8.

$$l(t) = (kDt)^{1/2} \tag{8}$$

In this equation k is a numerical nondimensional constant that is specified by experimental conditions. Equation 8 can be expressed in the form of Equation 9, which describes the change in area of a circular disk (diffusion zone), $S(t)$ with the same radius as the hemispherical nuclei.

$$S(t) = \pi l^2(t) = \pi kDt \tag{9}$$

If at t=0, N nanoparticles were present on the surface per unit area, then, the total size of the diffusion zones for all the nanoparticles on the surface of the bead at time, t is given by Equation 10.

$$\theta_{ex} = N\pi kDt \tag{10}$$

In this equation, θ_{ex} is the fraction of the area covered by the diffusion zones without taking overlap into account. If the N centers are randomly distributed on the surface of the bead, the actual fraction of area covered (which is smaller due to the overlap) can be related to θ_{ex}, by the Avrami equation $\theta = 1 - \exp(-\theta_{ex})$.

The coverage of the surface of the bead by the growing nanoparticles is thus given by Equation 11.

$$\theta = 1 - \exp(-N\pi kDt) \tag{11}$$

The radial flux density through the boundaries of the diffusion zones will be given by the equivalent planar diffusive flux to a surface of fractional area θ. Conservation of mass requires that the amount of material entering the diffusion zones be equal to the amount being incorporated into the growing nanoparticles (we assume that the interfacial kinetics is instantaneous). The mass current to the whole surface is therefore given by Equation 12.

$$\dot{m}_N = \frac{SMD^{1/2}c\theta}{\pi^{1/2}t^{1/2}} = \frac{SMD^{1/2}c}{\pi^{1/2}t^{1/2}}\left[1 - exp(-N\pi kDt)\right] \tag{12}$$

We define a 'characteristic time' $\tau = \frac{1}{N\pi kD}$ and the constant $C_1 = \frac{MD^{1/2}c}{\pi^{1/2}}$ and rewrite the equation for the mass current on the surface of the bead as Equation 13.

$$\dot{m}_N = \frac{SC_1}{t^{1/2}}\left[1 - \exp(-\frac{t}{\tau})\right] \tag{13}$$

The quantity that we are interested in, the mass of gold as a function of time is given by Equation 14.

$$m_N = \int_0^t \dot{m}_N \, \mathrm{d}t \tag{14}$$

At early times (small t), $t \ll \tau$, and $1 - \exp(-\frac{t}{\tau}) \simeq \frac{t}{\tau}$.

$$\begin{aligned} m_{N,t\ll\tau} &= \int_0^t \dot{m}_N \, \mathrm{d}t \\ &= \frac{SC_1}{\tau}\int_0^t t^{1/2} \, \mathrm{d}t \\ &= \frac{2SC_1}{3\tau}t^{3/2} \\ &= \frac{2}{3}NSMkcD^{3/2}\pi^{1/2}t^{3/2} \end{aligned} \tag{15}$$

When t is large, $t \gg \tau$, and and $1 - exp(-\frac{t}{\tau}) \simeq 1$

$$
\begin{aligned}
m_{N,t\gg\tau} &= \int_0^t \dot{m}_N \, \mathrm{d}t \\
&= SC_1 \int_0^t \frac{1}{t^{1/2}} \, \mathrm{d}t \\
&= 2SC_1 t^{1/2}
\end{aligned} \tag{16}
$$

An expression for k can be obtained by noting that the current for $t \to 0$ must be identical to that flowing to N isolated hemispherical nuclei [1–3], i.e. as described by Equation 7.

$$
k = (8\pi cM/\rho)^{1/2} \tag{17}
$$

By observing these two asymptotic limits, we observe that at early times, the number of nanoparticles on the surface of the bead is important, while at later times, when a film has formed on the surface the mass incorporation is akin to that of a planar surface. The characteristic time τ determines the cross over between when the particles can be modeled as independently growing nuclei to when their growth rate is affected by neighbors.

We also note that $\tau \propto \frac{1}{N}$. Thus for larger values of N, the growth rate of the nanoparticles will be affected by the presence of their neighbors sooner.

III. EQUILIBRIUM LEVITATION HEIGHT OF A BEAD IN THE MAGLEV

Following [4] the general form of the total potential energy density (energy per unit volume), u, of the MagLev system is given by Equation 18.

$$
\begin{aligned}
u &= u_{mag} + u_{grav} \\
&= -\frac{1}{2_{\mu o}} \Delta\chi(\vec{r})\vec{B}^2 - \Delta\rho(\vec{r})\vec{g} \cdot h
\end{aligned} \tag{18}
$$

In this equation, u_{mag} is the magnetic contribution and u_{grav} is the gravitational contribution to the total potential energy density, $\Delta\chi = \chi_o(\vec{r}) - \chi_s$ is the magnetic susceptibility of the object relative to a homogenous medium, $\Delta\rho(\vec{r}) = \rho_o(\vec{r}) - \rho_s$ is the density of the object relative to a homogenous medium, and $h = (0, 0, h)$ is the height of the object. In

general, the object can be heterogeneous in both density and magnetic susceptibility such that these functions depend on the position coordinate r. Note that taking the negative of the derivative of u_{grav} and u_{mag} with respect to z gives the magnetic and gravitational forces.

In a MADA a material that has different properties than the material that composes the bead is deposited onto the surface of the beads. The reactants are in vast excess in the developing buffer thus we assume that the magnetic susceptibility of the object and the medium does not change significantly throughout the course of a typical assay.

At static equilibrium, the potential energy, $U = \int_V u\, dV$, where V is the volume of the object, has to be minimized.

The equilibrium levitation height, h will occur where $\frac{\partial U}{\partial h} = 0$.

$$h = \frac{g\mu_o d^2}{4\Delta\chi B_o^2}(\rho - \rho_{buffer}) + \frac{d}{2} \tag{19}$$

IV. THE CHANGE IN DENSITY OF THE BEAD IN A MADA

Equation 20 gives the total mass of the bead a function of time in the developing buffer, $m_{tot}(t)$, and Equation 21 gives the density, $\rho_{tot}(t)$of the bead.

$$m_{tot}(t) = m_{bead} + m_N(t) = \rho_{bead}V + m_N(t) \tag{20}$$

$$\rho_{tot}(t) = \frac{\rho_{bead}V + m_N(t)}{V} \tag{21}$$

For equation 21 we made the assumption that the volume of the bead, $V \gg$ volume of the deposited metal.

Equation 22 gives the levitation height of the bead, due to the deposition of metal on the surface of the bead.

$$
\begin{aligned}
h(t) &= \frac{g\mu_o d^2}{4\Delta\chi B_o^2}\left(\rho_{tot}(t) - \rho_{buffer}\right) + \frac{d}{2} \\
&= \frac{g\mu_o d^2}{4\Delta\chi B_o^2}\left(\frac{\rho_{bead}V + m_N(t)}{V} - \rho_{buffer}\right) + \frac{d}{2} \\
&= \frac{g\mu_o d^2}{4\Delta\chi B_o^2}\left((\rho_{bead} - \rho_{buffer}) + \frac{m_N(t)}{V}\right) + \frac{d}{2} \\
&= \Phi_1' \frac{m_N(t)}{V} + \Phi_2
\end{aligned} \tag{22}
$$

For the final step we define two constants, $\Phi_1' = \frac{g\mu_o d^2}{4\Delta\chi B_o^2}$ and $\Phi_2 = \Phi_1'(\rho_{bead} - \rho_{buffer}) + \frac{d}{2}$.

Examining Equation 22 we see that for a bead that is density matched with the buffer, $\Phi_2 = \frac{d}{2}$.

At the start of the development period, we expect that levitation height should evolve according to Equation 23.

$$
h(t) = \Phi_1 N \frac{S}{V} t^{3/2} + \Phi_2 \tag{23}
$$

In this equation, $\Phi_1 = \frac{g\mu_o d^2 MkcD^{3/2}\pi^{1/2}}{6\Delta\chi B_o^2}$.

For a given t, $h(t)$ is larger for large N. Furthermore, $h(t)$ depends on the surface area to volume ratio, S/V. Thus everything else being equal, using particles of larger SA:V ratio should result in a more sensitive assay.

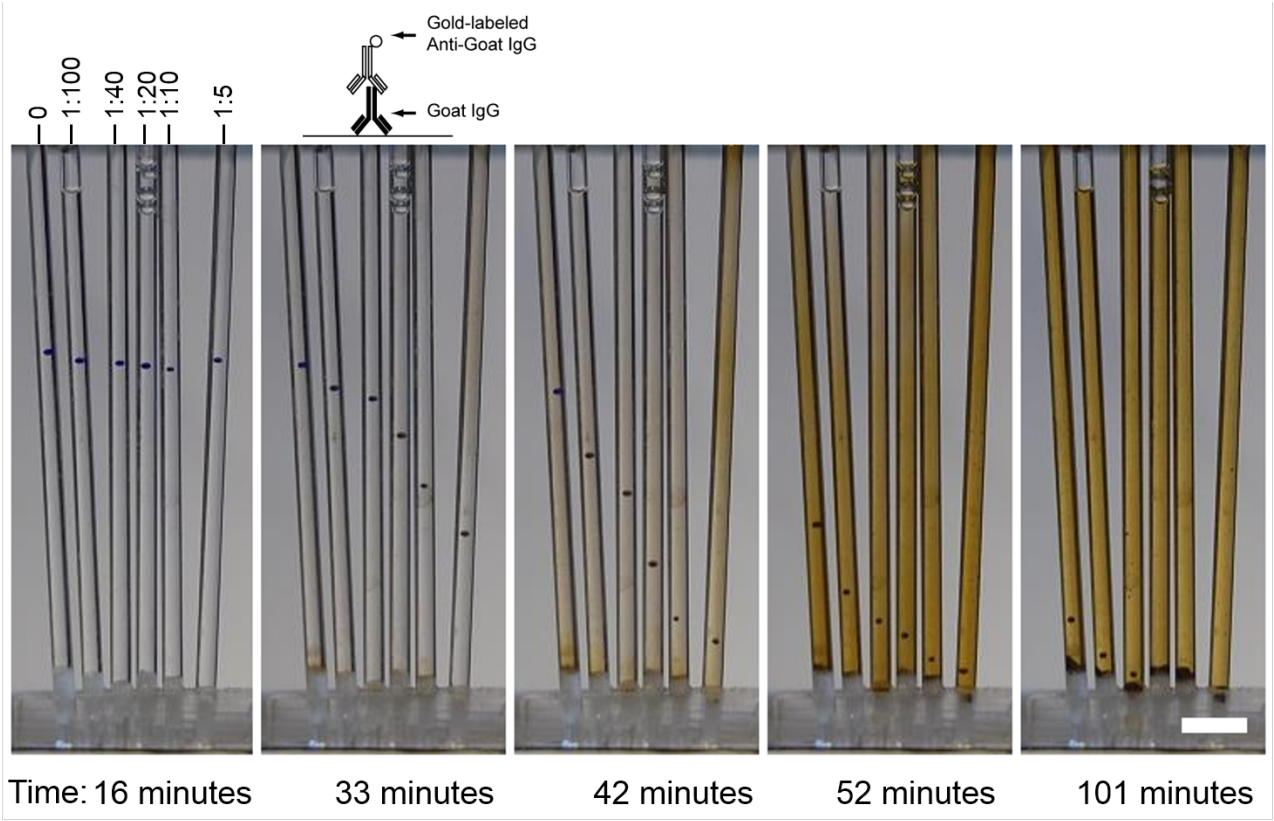

Fig. S3. Example of a silver metal-amplified density assay, AgMADA. Goat immunoglobulin G was immobilized covalently on the surface of the beads, which were colored blue. The beads were exposed to serial dilutions of 10-nm gold-labeled anti-goat IgG and then placed in a developing buffer prepared with a silver amplification reagent purchased form Sigma-Aldrich. Like the AuMADA, beads that were exposed to higher concentrations of gold-labeled proteins changed levitation height faster. Unlike gold amplification however, the electroless silver deposition bath was unstable, and eventually metallic silver precipitates from the solution, seen as the change in color of the solution to brown. Large precipitates sediment to the bottom of the capillary. The decrease in the concentration of silver ions decreases the density of the solution and hence all beads, including the bead that was not exposed to gold-labeled antibody, fall to the bottom of the capillary after 42 minutes. Scale bar 0.5 mm

---

[1] B. Scharifker and G. Hills, Electrochimica Acta **28**, 879 (1983).

[2] S. Fletcher, Journal of the Chemical Society-Faraday Transactions I **79**, 467 (1983).

[3] G. Gunawardena, G. Hills, I. Montenegro, and B. Scharifker, Journal of Electroanalytical Chemistry **138**, 225 (1982).

[4] A. Subramaniam, D. Yang, H.-D. Yu, A. Nemiroski, S. Tricard, A. Ellerbee, S. Soh, and G. Whitesides, Proceedings of the National Academy of Sciences **111**, 12980 (2014).

[5] D. M. Mock and P. Horowitz, *Methods in Enzymology, [25] Fluorometric assay for avidin-biotin interaction* (Academic Press, 1990), vol. 184.

[6] M. Wilchek and E. A. Bayer, *Methods in Enzymology, [2] Introduction to avidin-biotin technology* (Academic Press, 1990), vol. 184, pp. 5–13.

[7] T. Buranda, G. M. Jones, J. P. Nolan, J. Keij, G. P. Lopez, and L. A. Sklar, Journal of Physical Chemistry B **103**, 3399 (1999).

[8] S. C. Huang, M. D. Stump, R. Weiss, and K. D. Caldwell, Analytical Biochemistry **237**, 115 (1996).

[9] D. Wild, *The Immunoassay Handbook* (Elsevier Ltd., Oxford, 2005), 3rd ed.